Flow Turbulence Combust (2013) 90:401–418
DOI 10.1007/s10494-012-9425-9

Transition from Countergradient to Gradient Scalar Transport in Developing Premixed Turbulent Flames

A. N. Lipatnikov · V. A. Sabelnikov

Received: 28 February 2012 / Accepted: 5 November 2012 / Published online: 28 November 2012

Abstract A simple model of turbulent scalar flux developed recently by the present authors is applied to determine the direction of the flux in a statistically planar one-dimensional premixed flame that does not affect turbulence and has self-similar mean structure. Results obtained in the case of statistically stationary turbulence indicate that transition from countergradient to gradient turbulent scalar transport may occur during flame development, as the peak mean rate of product creation moves to the trailing edge of the flame brush. In the case of decaying turbulence, the opposite transition (from gradient to countergradient transport) was simulated in line with available DNS data. In both cases, transition instant depends strongly on turbulence and mixture characteristics. In particular, countergradient transport is suppressed by an increase in the rms turbulent velocity and by a decrease in the laminar flame speed or density ratio, in line with available experimental and DNS data. The obtained results lend qualitative support to the model of turbulent scalar flux addressed in the present work.

Keywords Premixed turbulent combustion · Countergradient scalar transport · Modeling

Mathematics Subject Classifications (2010) 80A25 · 76F25

A. N. Lipatnikov (✉)
Department of Applied Mechanics, Chalmers University of Technology,
Gothenburg, 41296, Sweden
e-mail: lipatn@chalmers.se

V. A. Sabelnikov
ONERA - The French Aerospace Lab., 91761 Palaiseau, France
e-mail: Vladimir.Sabelnikov@onera.fr

1 Introduction

As theoretically predicted by Prudnikov [1], Clavin and Williams [2], and Libby and Bray [3], experimentally discovered by Moss [4] and Tanaka and Yanagi [5], and documented in a number of subsequent papers; turbulent scalar flux $\overline{\rho \mathbf{u}'' c''}$ of the combustion progress variable c points to the trailing edges of many premixed turbulent flames. The phenomenon of a positive product $\overline{\rho \mathbf{u}'' c''} \cdot \nabla \bar{c}$ is commonly called "countergradient diffusion" or countergradient transport (CGT), while such a product is negative in the case of classical gradient diffusion (GD). Here, $\mathbf{u}$ is the flow velocity vector, ρ is the density, overlines and overbars designate the Reynolds average, e.g. $\bar{c}$ with $c' = c - \bar{c}$, and $\tilde{q} = \overline{\rho q}/\bar{\rho}$ is the Favre-averaged (or density-weighted) value of a scalar q with $q'' = q - \tilde{q}$.

As reviewed elsewhere [6], CGT was documented in many premixed turbulent flames, while gradient transport was also documented in many other premixed turbulent flames. By varying the equivalence ratio F, Kalt et al. [7, 8] obtained (i) CGT from near-stoichiometric methane- and propane-air Bunsen flames, but (ii) GD from lean flames. The data by Kalt et al. [9], who investigated 11 lean and stoichiometric, methane- and propane-air flames stabilized in impinging jets, indicate GD in five moderately turbulent flames, but CGT in one moderately turbulent flame and five weakly turbulent ones. Troiani et al. [10] documented CGT in near-stoichiometric open methane-air flames stabilized by a bluff body, whereas the behavior of the flux $\overline{\rho \mathbf{u}'' c''}$ was gradient in a lean flame ($F = 0.67$). Furthermore, both regions with GD and regions with CGT were observed in the same flame, e.g. in a confined flame stabilized by a rod [11], or in open flames stabilized by bluff bodies [10, 12], or in a swirl-stabilized flame [13].

Such experimental data as briefly reviewed above call for a criterion that would allow a researcher to predict the direction of turbulent scalar flux under particular conditions. The first criterion of that kind was proposed to be used by Bray [14, 15] who argued that turbulent scalar flux shows the countergradient (gradient) behaviour if the following ratio

$$N_B = \frac{\tau S_L}{2\alpha u'}, \tag{1}$$

called "Bray number" later, is larger (lower) than unity. Here, S_L is the laminar flame speed, $\tau = \sigma - 1$ is the heat-release factor, $\sigma = \rho_u/\rho_b$ is the density ratio, u' is the rms turbulent velocity, and α is an empirical parameter that was hypothesized [15] to be an increasing function of a ratio L/δ_L of the integral turbulence length scale L to the laminar flame thickness $\delta_L = \kappa_u/S_L$, where κ_u is the heat diffusivity of the unburned mixture.

After the pioneering work by Bray et al. [14, 15], a criterion of transition from GD to CGT received plenty of attention in the literature and several physical mechanisms that affect the transition were studied [14–27]. In particular, by processing the results of direct numerical simulation (DNS) by Trouvé and Poinsot [28], Swaminathan et al. [17] mentioned that the development of premixed turbulent flame may affect the transition referred to. Later, Zimont et al. [20, 22] and Lipatnikov and Chomiak [21, 24] hypothesized that the flame development is one of the key factors that control the direction of turbulent scalar flux in premixed combustion.

In a recent paper [27], the following criterion

$$\Upsilon \equiv \frac{1}{u_t}\frac{\mathrm{d}\delta_t}{\mathrm{d}\theta} = \frac{U_{t,\infty}}{u'}\Psi. \tag{2}$$

of the discussed transition was derived by theoretically analyzing the balance equations for the mass and combustion progress variable, see Eqs. 6 and 7 in the next section, in the case of a statistically planar 1D premixed flame that propagates in frozen turbulence and has a self-similar mean structure. CGT (GD) is associated with a lower (larger) left hand side (LHS) of Eq. 2, as compared with the right hand side (RHS). Here, $U_{t,\infty} = U_t(t \to \infty)$ is a fully-developed turbulent burning velocity, $u_t = U_t/U_{t,\infty} = \int_{-\infty}^{\infty} \omega d\xi$ and $\delta_t = \Delta_t/L$ are the normalized burning velocity and mean flame brush thickness, respectively, $\theta = t/\tau_t$ is the normalized time, $\tau_t = L/u'$ is a time scale of turbulence, $\omega = \Delta_t\overline{\Omega}/U_{t,\infty}$ is the normalized mean mass rate of product creation $\overline{\Omega}$, i.e. the source term in the $\tilde{c}$-balance Eq. 7 discussed later,

$$\Psi \equiv \rho_u \frac{\int_{-\infty}^{\infty}(1-2\tilde{c})\,\overline{\Omega}\mathrm{d}\xi}{\int_{-\infty}^{\infty}\overline{\Omega}\mathrm{d}\xi\int_{-\infty}^{\infty}\bar{\rho}\tilde{c}\,(1-\tilde{c})\,\mathrm{d}\xi} = \rho_u \frac{\int_{-\infty}^{\infty}(1-2\tilde{c})\left(\omega - \frac{\mathrm{d}\tilde{c}}{\mathrm{d}\xi}\right)\mathrm{d}\xi}{\int_{-\infty}^{\infty}\omega\mathrm{d}\xi\int_{-\infty}^{\infty}\bar{\rho}\tilde{c}\,(1-\tilde{c})\,\mathrm{d}\xi}, \tag{3}$$

ρ_u is the density of unburned mixture, and

$$\xi = \frac{x - x_f(t)}{\Delta_t(t)} \tag{4}$$

is the normalized spatial distance x, where $x_f(t)$ is mean flame position. The assumption of self-similarity, well supported by numerous experimental data analyzed elsewhere [29, 30], means that $\tilde{c}(x,t)$ and $\bar{\rho}(x,t)$ depend on a single variable ξ, rather than on two independent variables x and t.

The criterion given by Eq. 2 highlights the influence of flame development on the direction of turbulent scalar flux. Indeed, due to an increase in the burning velocity and a decrease in the growth rate $\mathrm{d}\delta_t/\mathrm{d}\theta$ as a flame develops [29], the factor Υ decreases with time. Consequently, solely transition from GD to CGT is possible if Ψ is positive and does not depend (or depend weakly) on time. This conclusion is valid for any model of turbulent scalar flux that is consistent with the self-similarity of the mean flame structure. For instance, if (i) the following expression

$$\overline{\Omega} = \frac{\psi}{\tau_f}, \qquad \psi = \psi(\bar{c},\tau) \geq 0, \qquad \psi(\bar{c}=0) = \psi(\bar{c}=1) = 0, \tag{5}$$

which subsumes various models for the mean rate of product creation [31], is invoked and (ii) the flame time scale $\tau_f = \tau_f(u', L, S_L, \delta_L, t, \ldots)$ depends neither on $\tilde{c}$ nor on x; then, Ψ does not depend on flame-development time. Therefore, if GD dominates during an early stage of flame development, characterized by a large Υ, and, moreover, $\Psi > 0$, i.e. if the maximum of $\omega(\tilde{c})$ is shifted to the leading edge; then, transition from GD to CGT occurs at certain normalized transition time θ_{tr} due to a decrease in $\Upsilon(\theta)$.

The opposite transition (from CGT, which dominates at $\theta < \theta_{tr}$, to GD, which dominates at $\theta > \theta_{tr}$) seems also to be admissible provided that the peak of the $\omega(\tilde{c})$-curve moves to the burned side of developing turbulent flame brush and,

therefore, Ψ decreases with time or even becomes negative at certain θ. The main goal of the present paper is to show that such a hypothetical scenario, which was never discussed in the literature, to the best of the authors' knowledge, is feasible.

Another goal of our work is to qualitatively test a simple model for evaluating the normal (to the mean flame brush) component of $\overline{\rho \mathbf{u}'' c''}$, see Eqs. 10 and 11 in the next section, that was recently developed and validated [32, 33] against experimental data obtained from flames stabilized in impinging jets.

In the next section, the problem is stated. An analytical solution is reported in the third section. Results are discussed in the fourth section, followed by conclusions.

2 Statement of the Problem

Let us consider a statistically planar one-dimensional developing premixed turbulent flame that propagates from right to left in frozen turbulence. The flame expansion and mean structure are described by the following well-known Favre-averaged mass

$$\frac{\partial \bar{\rho}}{\partial t} + \frac{\partial}{\partial x}(\bar{\rho}\tilde{u}) = 0 \tag{6}$$

and combustion progress variable

$$\bar{\rho}\frac{\partial \tilde{c}}{\partial t} + \bar{\rho}\tilde{u}\frac{\partial \tilde{c}}{\partial x} = -\frac{\partial}{\partial x}\overline{\rho u'' c''} + \rho_u \overline{\Omega} \tag{7}$$

balance equations. Here, t is time, x is spatial coordinate, u is the x-component of the flow velocity vector. Let us assume that the following well-known BML expressions [3, 34]

$$\rho_b \bar{c} = \bar{\rho}\tilde{c} = \rho_u \frac{\tilde{c}}{1 + \tau \tilde{c}}, \tag{8}$$

$$\begin{aligned} \overline{\rho u'' c''} &= \bar{\rho}\tilde{c}(1-\tilde{c})(\bar{u}_b - \bar{u}_u) = \bar{\rho}(1-\tilde{c})(\tilde{u} - \bar{u}_u) \\ &= \rho_u(1-\bar{c})(\tilde{u} - \bar{u}_u) = \frac{\rho_u \rho_b}{\bar{\rho}}(1-\bar{c})(\bar{u} - \bar{u}_u) \end{aligned} \tag{9}$$

hold. Here, subscripts u and b relate to quantities conditioned on unburned and burned mixture, respectively.

The transport term on the RHS of Eq. 7 is closed invoking the following relation

$$(1-\bar{c})\nabla \cdot \tilde{\mathbf{u}}_u = b u' \overline{|\nabla c|} = b u' \overline{\Sigma} = \frac{b u'}{S_L}\overline{\Omega}, \tag{10}$$

$$b = b_0 \frac{(1-\bar{c})^q}{(1 + u'/S_L)^p}, \tag{11}$$

obtained and validated recently by the the present authors [32, 33]. Here, $\overline{\Sigma}$ is flame surface density, u' is the rms turbulent velocity at the leading edge of turbulent flame brush, q, p, and $b_0 = b_0(q, p)$ are constants. Results reported in the following were computed using $q = p = 0.5$ and $b_0 = 2.43$ [33] if the opposite is not specified. The current study is particularly aimed at further assessing Eqs. 10 and 11.

As regards the mean rate $\overline{\Omega}$, there are two alternative ways of evaluating it. The simplest one consists of using a known closure relation, as done in [27] when investigating another model of turbulent scalar flux. However, because all available algebraic closure relations for $\overline{\Omega}$ are subsumed by Eq. 5, as discussed elsewhere [31], this way will not lead us to results that differ substantially from results yielded by Eq. 2 with a time-independent Ψ and already considered elsewhere [27]. Moreover, this way will not allow us to draw solid conclusions about Eqs. 10 and 11, because eventual disagreement between results computed by us and available experimental and DNS data may be caused by the limitations of the invoked model of $\overline{\Omega}$, as well as eventual agreement may result from the cancellation of errors inherent in Eq. 10 and the latter model.

For these reasons, another way of investigating eventual transition from CGT to GD and assessing Eq. 10 was chosen by us. The mean flame speed, thickness, and structure were assumed to be known, while $\overline{\rho u'' c''}$ and $\overline{\Omega}$ were computed by substituting a prescribed $\bar{c}(x,t)$ into Eqs. 7–11. Subsequently, the obtained profiles of $\overline{\rho u'' c''}(x,t)$ and $\overline{\Omega}(x,t)$ were analyzed in order to determine the direction of turbulent scalar flux and to assess Eqs. 10 and 11 by comparing the predicted trends with the contemporary knowledge on the behaviour of the turbulent scalar flux and the mean reaction rate in premixed turbulent flames. The present article is restricted to the computed profiles of $\overline{\rho u'' c''}(x,t)$, while the behaviour of the mean rate $\overline{\Omega}(x,t)$ is addressed in an accompanying paper [33].

Such a method is favored by the fact that the mean structure of numerous premixed turbulent flames is well parametrized by the following self-similar profile [29, 30]

$$\bar{c} \;=\; 1 \;-\; \frac{1}{2}\,\mathrm{erfc}\left(\xi\sqrt{\pi}\right) \;=\; 1 \;-\; \sqrt{\frac{1}{\pi}}\int_{\xi\sqrt{\pi}}^{\infty} \mathrm{e}^{-\zeta^2}\,\mathrm{d}\zeta. \tag{12}$$

To investigate the sensitivity of computed results to the chosen self-similar profile of $\bar{c}(\xi)$, simulations were also performed using another widely used parametrization [35]

$$\bar{c} = \frac{1}{1+\mathrm{e}^{-4\xi}}. \tag{13}$$

Because results obtained using either Eq. 12 or Eq. 13 were always qualitatively similar, only the former results will be reported in the present paper.

To close the problem, the $\Delta_t(t)$ and $x_f(t)$ in Eq. 4 should be modeled. Because the mean thickness of many turbulent premixed flames grows by the turbulent diffusion law [1, 29], we invoked the following expression

$$\Delta_t^2 = 4\pi\, L^2\theta\left[1-\theta^{-1}\left(1-\mathrm{e}^{-\theta}\right)\right]. \tag{14}$$

It is worth remembering that Eq. 14 does not hold at $\theta \gg 1$ and, probably, at $u' \ll S_L$.

The following analysis will be performed in the coordinate framework attached to the mean flow of the unburned mixture, i.e. $\bar{u}(-\infty) = 0$. In this framework,

$$x_f = x_f(t=0) - \int_0^t U_t(\vartheta)\mathrm{d}\vartheta, \tag{15}$$

with the time-dependent turbulent burning velocity $U_t(t)$ being an input parameter of the problem. The following expression

$$U_t = S_L + C_U u' Da^{1/4} \left[1 + \theta^{-1}\left(\mathrm{e}^{-\theta} - 1\right)\right]^{1/2}, \tag{16}$$

discussed in detail elsewhere [29], was invoked. Here, $Da = \tau_t/\tau_c$ is the Damköhler number, $\tau_c = \delta_L/S_L$ is the chemical time scale, and $C_U = 0.4$ is a constant.

3 Solution

Substitution of a $\tilde{c}(\xi)$ into Eq. 6 followed by integration from $-\infty$ to ξ yields

$$\tilde{v} = \frac{\rho_u}{\bar{\rho}} - 1 + \frac{\Gamma}{\bar{\rho}} \int_{-\infty}^{\xi} \zeta \frac{\mathrm{d}\bar{\rho}}{\mathrm{d}\zeta} \mathrm{d}\zeta = \frac{\rho_u}{\bar{\rho}} - 1 + \frac{\tau \Gamma \rho_u}{2\pi(1+\tau)\bar{\rho}} \mathrm{e}^{-\pi\xi^2} \tag{17}$$

using Eq. 12. Here, $v \equiv u/U_t$ is the normalized velocity and

$$\Gamma \equiv \frac{1}{U_t} \frac{d\Delta_t}{dt}. \tag{18}$$

To find a solution for the velocity $\bar{u}_u$ conditioned on unburned mixture, let us rewrite Eq. 7 in the following form [36, 37]

$$\frac{\partial}{\partial x}\left[(1-\bar{c})\,\bar{u}_u\right] = \frac{\partial \bar{c}}{\partial t} - \overline{\Omega} \tag{19}$$

using Eqs. 6, 8, and 9. Substitution of a $\bar{c}(\xi)$ and Eq. 10 into Eq. 19 yields

$$\frac{\partial \bar{v}_u}{\partial \xi} = \frac{\mathrm{d}\bar{c}}{\mathrm{d}\xi} \frac{\bar{v}_u + 1 - \Gamma\xi}{(1+s_L)(1-\bar{c})}, \tag{20}$$

where $s_L = S_L/(bu')$ depends on $\bar{c}$ by virtue of Eq. 11. One can easily check by substitution that Eq. 20 supplemented with the boundary condition of $\bar{v}_u(-\infty) = \bar{v}(-\infty) = 0$ has the following analytical solution

$$\begin{aligned} \bar{v}_u &= \underbrace{\mathrm{e}^G \int_{-\infty}^{\xi} \frac{1}{(1+s_L)(1-\bar{c})} \mathrm{e}^{-G} \frac{\mathrm{d}\bar{c}}{\mathrm{d}\zeta} \mathrm{d}\zeta}_{\bar{v}_u^{(1)}} - \Gamma \underbrace{\mathrm{e}^G \int_{-\infty}^{\xi} \frac{\zeta}{(1+s_L)(1-\bar{c})} \mathrm{e}^{-G} \frac{\mathrm{d}\bar{c}}{\mathrm{d}\zeta} \mathrm{d}\zeta}_{\bar{v}_u^{(2)}} \\ &= \bar{v}_u^{(1)} - \Gamma \bar{v}_u^{(2)}, \end{aligned} \tag{21}$$

where

$$G = \int_{-\infty}^{\xi} \frac{1}{(1+s_L)(1-\bar{c})} \frac{\mathrm{d}\bar{c}}{\mathrm{d}\zeta} \mathrm{d}\zeta = \int_0^{\bar{c}} \frac{\mathrm{d}\bar{c}}{(1+s_L)(1-\bar{c})}. \tag{22}$$

Note that Eq. 21 could yield CGT in the case of a constant density. Indeed, if the second term on the RHS is larger than the first term, i.e. $\Gamma\bar{v}_u^{(2)} > \bar{v}_u^{(1)}$, then, $\bar{v}_u$ given by Eq. 21 could be negative. In such a case, both $\bar{v}_b$ and $\overline{\rho v''c''}$ could be positive by virtue of Eq. 9 and because $\bar{v} = 0$ in the selected coordinate framework. However, in our simulations, negative $\bar{v}_u$ was never obtained, because (i) the integral that determines $\bar{v}_u^{(2)}$ involves ζ in the fraction and is negative at lower $\bar{c}$, hence, (ii) the condition of $\Gamma\bar{v}_u^{(2)} > \bar{v}_u^{(1)}$ could only be satisfied if $\bar{c}$ is sufficiently close to unity, but (iii) Eq. 12 or Eqs. 13 and 21 yield $\bar{v}_u^{(2)} \ll \bar{v}_u^{(1)}$ when $\bar{c}$ is close to unity, while (iv) the parameter Γ determined by Eqs. 14, 16, and 18 is bounded, i.e. $\Gamma \leq u'/S_L$.

It is worth stressing that eventual (if $\Gamma \to \infty$) CGT at the trailing edge of a constant-density "flame" results from combining Eq. 10 with either Eq. 12 or Eq. 13. If neither Eq. 12 nor Eq. 13 is invoked, then, the model Eq. 10 does not suffer from this limitation and offers an opportunity to straightforwardly relate $\bar{\mathbf{u}}$ and $\bar{\mathbf{u}}_u$ in a general 3D case. Indeed,

$$\begin{aligned}\nabla\cdot\bar{\mathbf{u}} &= \nabla\cdot\tilde{\mathbf{u}} + \frac{\tau}{\rho_u}\nabla\cdot\overline{\rho\mathbf{u}''c''} = -\frac{1}{\bar{\rho}}\frac{\partial\bar{\rho}}{\partial t} - \frac{\tilde{\mathbf{u}}}{\bar{\rho}}\nabla\bar{\rho} + \frac{\tau}{\rho_u}\nabla\cdot\overline{\rho\mathbf{u}''c''} \\ &= \frac{1}{\rho_u}\left[\tau\bar{\rho}\frac{\partial\tilde{c}}{\partial t} + \tau\bar{\rho}\tilde{\mathbf{u}}\cdot\nabla\tilde{c} + \tau\nabla\cdot\overline{\rho\mathbf{u}''c''}\right] = \tau\overline{\Omega}\end{aligned} \tag{23}$$

by virtue of Eqs. 8 and 9. Equations 10 and 23 result in

$$\nabla\cdot\bar{\mathbf{u}} - \nabla\cdot\bar{\mathbf{u}}_u = \left(\tau - \frac{bu'}{S_L(1-\bar{c})}\right)\overline{\Omega}. \tag{24}$$

In the case of a constant density, $\tau = 0$ and the RHS of Eq. 24 is negative. Accordingly, the LHS is also negative. Consequently, in the 1D flame under consideration, the model Eq. 10 yields the gradient behavior of the turbulent scalar flux (i.e. $\bar{u} = 0$, $\bar{u}_u(\bar{c} > 0) > 0$, and $\bar{u}_b < 0$, because $(1-\bar{c})\bar{u}_u + \bar{c}\bar{u}_b = \bar{u} = 0$) everywhere within the flame brush. If either Eq. 12 or Eq. 13 is also invoked, then, Eq. 24 holds, but $\overline{\Omega}$ could be negative at $\bar{c} \to 1$ if $\Gamma \to \infty$.

In the case of a variable density, Eq. 24 shows that a necessary condition for observing CGT within the turbulent flame brush is as follows

$$\frac{\tau S_L}{bu'} > 1, \tag{25}$$

similarly to the Bray-number criterion. However, even if Eq. 25 holds, the flux $\overline{\rho u''c''}$ can show the gradient behavior at larger $\bar{c}$, because the magnitude of the second term in the parentheses on the RHS of Eq. 24 increases with $\bar{c}$. Note that Eq. 24 indicates that CGT can occur even at the leading edge of a turbulent flame brush, contrary to common belief that turbulent scalar transport always shows the gradient behavior at $\bar{c} \to 0$. This issue is discussed elsewhere [38, 39]. Here, we restrict ourselves to mentioning that the model Eq. 10 has been obtained in the asymptotic case of infinitely thin instantaneous flame front and, therefore, Eq. 24 does not allow for the contribution of molecular diffusion to the flux of $\bar{c}$.

4 Results and Discussion

Here, we restrict ourselves solely to analyzing the behaviour of the normalized flux $\overline{\rho v'' c''}/\rho_u$, while the simulated profiles of the normalized rate ω are reported in the accompanying paper [33]. For flames simulated here, $\partial\bar{c}/\partial x \geq 0$ and CGT (GD) is associated with positive (negative) flux.

Figure 1 indicates that CGT (GD) dominates at a low (high) ratio of u'/S_L at various θ. If the ratio of u'/S_L is moderate (see Fig. 1b), the flux shows the CGT behaviour in the largest part of flame brush during an early stage of flame development. As θ increases, the maximum value of $\overline{\rho v'' c''}$ decreases, the range of $\bar{c}$ characterized by $\overline{\rho v'' c''} > 0$ becomes narrower, but the magnitude of GD grows.

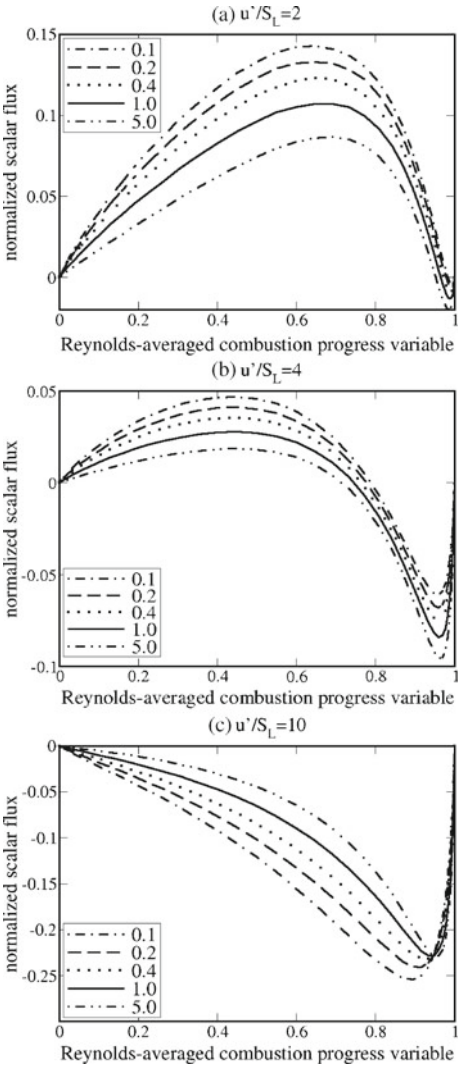

Fig. 1 Dependencies of the normalized flux $\overline{\rho v'' c''}/\rho_u$ on the Reynolds-averaged combustion progress variable $\bar{c}$, calculated at various normalized flame development times θ, specified in legends, and various ratios of u'/S_L, specified in headings

Such an evolution of the flux implies transition from CGT to GD during premixed turbulent flame development.

Shown in Fig. 2 is the evolution of the following three integral criteria

$$\int_{-\infty}^{\infty} \overline{\rho v'' c''} \mathrm{d}\zeta = 0 \tag{26}$$

$$\int_{0}^{1} \overline{\rho v'' c''} \mathrm{d}\bar{c} = 0, \tag{27}$$

$$\int_{0}^{1} \overline{\rho v'' c''} \mathrm{d}\tilde{c} = 0. \tag{28}$$

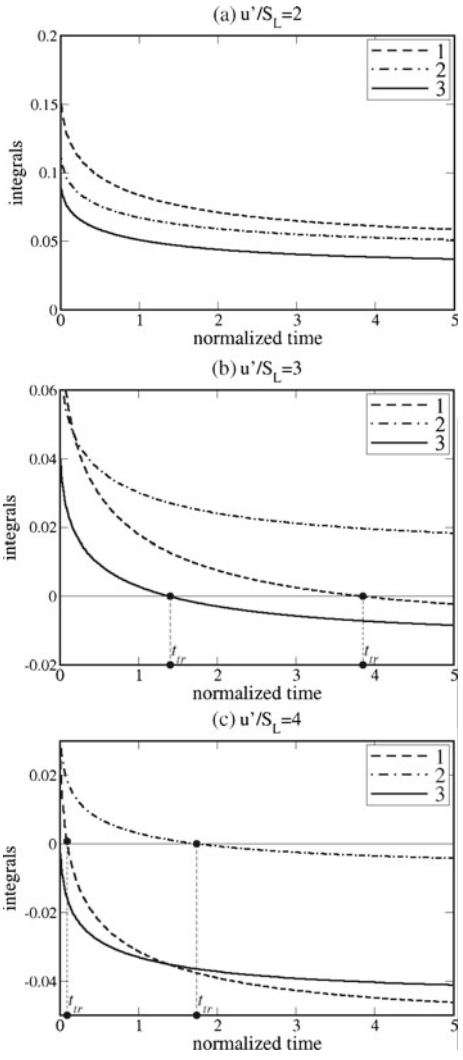

Fig. 2 Dependencies of various integral criteria on $\theta = t/\tau_t$, calculated at $u'/S_L = 2$ (**a**), 3 (**b**), and 4 (**c**). 1 - Eq. 26, 2 - Eq. 27, 3 - Eq. 28

In the case studied in the present paper, CGT (GD) is associated with positive (negative) integrals. If a ratio of $\tau S_L/u'$ is substantially larger than unity, then, the integrals are large during an early stage of flame development and decrease with time (see Fig. 2a and b). If the ratio is too large, then the integrals remain positive (see Fig. 2a), i.e. CGT dominates at any θ. If the ratio is moderately large, then, the integrals change their signs at certain transition instants θ_{tr} (see Fig. 2b) and transition from CGT to GD occurs.

As regards the direction of the discussed transition, the results of the present simulations are opposite to the recent numerical data reported by one of the present authors [27]. In the cited paper, the transition from GD to CGT was simulated by invoking Eq. 5, which is associated with a time-independent shape of $\omega(\xi)$-curve and a time-independent Ψ-factor defined by Eq. 3. In the present simulations, however, the shape of $\omega(\xi)$-curve depends on time and the Favre-averaged combustion progress variable $\tilde{c}_{\max}$ associated with the maximum of $\omega(\xi)$ increases with time (see Fig. 3a). Moreover, the magnitude of $\tilde{c}_{\max}$ is increased not only by θ, but also by u'/S_L and the latter effect is consistent with available DNS data, as discussed in the accompanying paper [33]. Due to the increase in $\tilde{c}_{\max}$ by θ and u'/S_L, the Ψ-factor decreases with time (see Fig. 3b) and may become negative if u'/S_L is sufficiently large. According to the criterion given by Eq. 2, small positive or any negative value of Ψ is associated with GD. Therefore, transition from CGT to GD may occur due to a decrease in Ψ with θ in the present simulations.

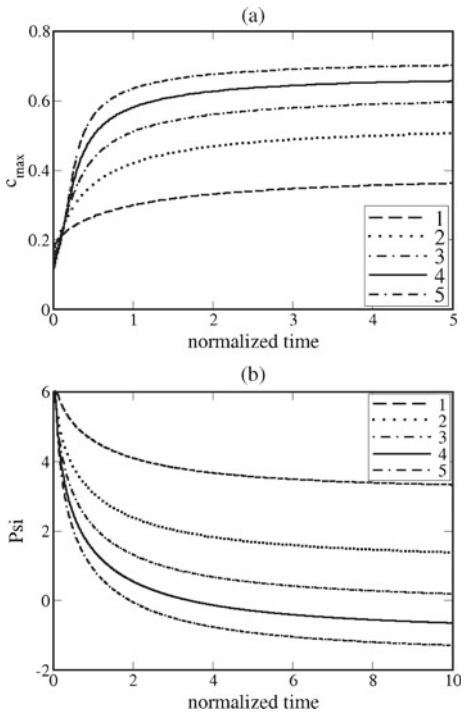

Fig. 3 Dependencies of **a** the Favre-averaged combustion progress variable $\tilde{c}_{\max}$ associated with the maximum of $\overline{\Omega}(\tilde{c})$ and **b** the Ψ-ratio given by Eq. 3 on the normalized flame development time, calculated at various u'/S_L specified in legends

The fact that the present model yields the well-pronounced dependence of the shape of $\omega(\xi)$- or $\omega(\tilde{c})$-curve on u'/S_L is of importance for the following reasons [27]. Integration of Eq. 7 from the leading edge of flame brush yields

$$\overline{\rho u'' c''} = \rho_u U_{t,\infty} \int_{-\infty}^{\xi} \left(\omega - \frac{\mathrm{d}\tilde{c}}{\mathrm{d}\zeta} \right) \mathrm{d}\zeta \tag{29}$$

in a hypothetical case of a fully-developed, statistically planar, 1D premixed flame that propagates in frozen turbulence. Equation 29 shows that the direction of turbulent scalar flux is controlled by the behavior of two curves, ω and $\mathrm{d}\tilde{c}/\mathrm{d}\xi$ as functions of $\tilde{c}$ [20]. If the shape of the $\omega(\tilde{c})$-curve does not depend on u'/S_L, then, the scalar transport in the considered flame may show either the gradient behaviour for any u'/S_L or the countergradient behaviour for any u'/S_L, i.e. transition from CGT to GD with decreasing the Bray number is impossible in the hypothetical case referred to. To the contrary, the 2D DNS data by Veynante et al. [15] indicate transition from GD to CGT if $u'_0/S_L = 2$ or 3, but do not indicate such a transition if $u'_0/S_L = 10$. Furthermore, Fig. 11 in the cited paper shows that the LHS of Eq. 26 is always negative even at $u'_0/S_L = 5$, i.e. GD dominates in that flame (although CGT is also observed in the middle of the flame brush at certain θ, see Fig. 10c in the cited paper). These results imply that ω depends differently on $\tilde{c}$ at different u'/S_L. Certainly, such a difference may be attributed to an eventual u'/S_L-dependence of the influence of combustion on turbulence, but this hypothesis has never been investigated to the best of the authors' knowledge. The present simulations offer an alternative explanation of the discussed DNS data by highlighting the inherent dependence of the shape of the $\omega(\tilde{c})$-curve on u'/S_L and θ.

Shown in Fig. 4a and b are the dependencies of the normalized and dimensional transition times, respectively, on u'. Although the calculated numbers depend strongly on the criterion used, all the three criteria yield the same trends; (i) a strong reduction in both θ_{tr} and t_{tr} by u', (ii) an increase in the dimensional transition time by turbulence length scale (cf. open and filled symbols in Fig. 4b), but (iii) a decrease in the normalized transition time with increasing L (cf. open and filled symbols in Fig. 4a). Because the present paper is aimed at discussing trends, rather than numbers, we will restrict ourselves to reporting results obtained using Eq. 26 in the following.

Figure 4c shows dependencies of θ_{tr} on the simplified Bray number $N'_B \equiv \tau S_L/u'$, computed by varying either u' (circles, triangles, and squares), or S_L (crosses and pluses), or the density ratio (diamonds and stars). Although θ_{tr} is increased by N'_B in all computed cases, θ_{tr} is not a single-valued function of N'_B. The former trend means that CGT is promoted by an increase N'_B, in line with the Bray-number criterion. However, the latter trend indicates that the use of time-independent N_B as a universal criterion for determining the direction of turbulent scalar flux oversimplifies the problem.

Let us compare the above numerical results with available experimental and DNS data. First, Fig. 4c implies that we may observe GD ($t > t_{tr}$) in lean flames characterized by a lower τS_L and, hence, by a shorter t_{tr}, but CGT ($t < t_{tr}$) in near-stoichiometric flames characterized by a higher τS_L and, hence, a longer t_{tr} provided that flame-development time is weakly affected by the variations in S_L and τ. Such a trend is consistent with the experiments by Kalt et al. [7], Frank et al. [8], and Troiani et al. [10]. The Sydney group [7, 8] measured turbulent scalar fluxes in various

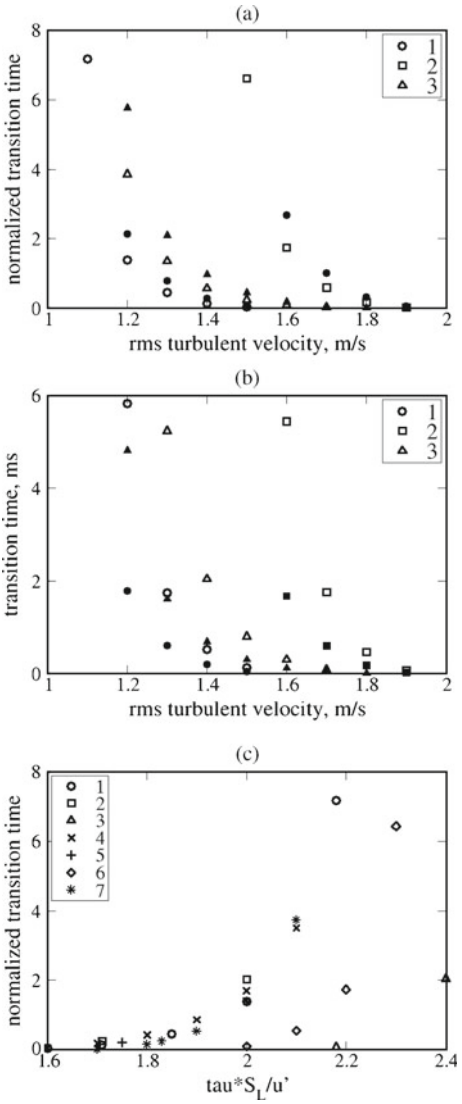

Fig. 4 Dependencies of normalized (**a**) and dimensional (**b**) transition time on rms turbulent velocity u'. 1 - Eq. 28, 2 - Eq. 27, 3 - Eq. 26. *Open* and *filled symbols* show results calculated at $L = 1$ and 5 mm, respectively. (**c**) Dependencies of θ_{tr} on a ratio of $\tau S_L/u'$ calculated by varying either u' (1–3), or S_L (4–5), or τ (6–7).
1 - $S_L = 0.4$ m/s, $\tau = 6$;
2 - $S_L = 0.1$ m/s, $\tau = 6$;
3 - $S_L = 0.4$ m/s, $\tau = 3$;
4 - $u' = 0.6$ m/s, $\tau = 6$;
5 - $u' = 1.2$ m/s, $\tau = 6$;
6 - $u' = 0.8$ m/s, $S_L = 0.4$ m/s;
7 - $u' = 1.2$ m/s, $S_L = 0.4$ m/s

Bunsen flames at fixed distance from the burner exit. When the equivalence ratio F was varied in the same oncoming flow, $|\bar{u}_b|$ was lower than $|\bar{u}_u|$ indicating GD in the leanest flames D ($F = 0.6$) characterized by the lowest product τS_L, whereas $|\bar{u}_b|$ was higher than $|\bar{u}_u|$ indicating CGT in other flames characterized by a larger τS_L. Troiani et al. [10] documented CGT from near-stoichiometric open methane-air flames stabilized by a bluff body, whereas the behavior of the flux $\overline{\rho u'' c''}$ was gradient in a lean flame ($F = 0.67$). Because neither oncoming turbulence characteristics, nor the flame-development time were substantially varied in these experiments, the observed transition from GD to CGT with the enrichment of lean mixtures is consistent with the computed trend shown in Fig. 4c.

It is worth noting that another model of turbulent scalar flux, developed by Zimont and Biagioli [22], was applied by them to simulating the aforementioned experiments by Frank et al. [8]. In the cited paper, GD (CGT) was reported in the leanest (richest) flame D (E), in qualitative agreement with the measured data. Furthermore, the recent numerical results reported by one of the present authors [27], which were obtained invoking a time-independent $\omega(\xi)$, also yielded the transition from GD to CGT with the enrichment of lean mixtures, but the computed effect of N'_B on the direction of turbulent scalar flux was caused by an acceleration of the transition from GD to CGT in a developing flame. Therefore, the experimental data by Kalt et al. [7], Frank et al. [8], and Troiani et al. [10] are qualitatively consistent not only with the present study, but also with other models [22, 27], even if these models result in the transition from GD to CGT in a developing flame and this transition is opposite to the transition from CGT to GD, shown in Fig. 2. Moreover, the simple Bray-number criterion given by Eq. 1, which does not allow for flame development, is also consistent with the experimental observation referred to.

Second, Fig. 4b implies that we may observe GD ($t > t_{tr}$) in flames characterized by a higher u' and, hence, by a shorter t_{tr}, but CGT ($t < t_{tr}$) in flames characterized by a lower u' and, hence, a longer t_{tr}. Such a trend is consistent with the experiments by Kalt et al. [7] and Frank et al. [8], who increased u' in the oncoming flow by moving a grid that generated turbulence towards the burner exit. Such measurements were performed in lean ($F = 0.7$) natural gas-air [8] and propane-air [7] flames. For both fuels, the increase in u' substantially reduced the magnitude of the slip velocity $\Delta u \equiv \bar{u}_b - \bar{u}_u$ with $|\bar{u}_b| > |\bar{u}_u|$ in all the cases referred to. Thus, these experimental data are associated with the transition from CGT to GD with increasing u', in line with the trend shown in Fig. 4b.

Finally, Figs. 1 and 2 indicate that, under moderately large values of $\tau S_L/u'$, transition from CGT to GD may occur during premixed turbulent flame development. Certain experimental [11–13] and DNS [15–17, 26, 40] studies do show that the direction of turbulent scalar flux may reverse in premixed flames. However, the majority of the cited studies imply the opposite transition, i.e. transition from GD to CGT during flame development. This inconsistency between our simulations, which indicate the transition from countergradient to gradient turbulent scalar transport, and the cited experimental and DNS studies, which show the opposite transition, might be associated with limitations of the present model. However, such a conclusion appears to be too hasty for the following reasons.

First, in the flames experimentally investigated by Veynante et al. [11] and Pfadler et al. [13], only axial scalar fluxes reversed direction with distance from flame-stabilization zones, while transverse fluxes showed either solely the gradient [11] or solely the countergradient [13] behaviour in all points where the measurements were performed. Because the mean flame brushes were almost parallel to the axial directions in these two cases, the transverse flux is much more proper for assessing the present model and there is no inconsistency between the behaviour of the measured transverse fluxes and the model predictions. Similarly, only the axial scalar flux reversed direction in the DNS of a V-shaped flame by Domingo et al. [40], while the transverse flux was either small (at a lower u'/S_L) or showed the gradient behaviour (see Fig. 9 in the cited paper).

Second, the data by Most et al. [12] indicate transition from CGT to GD, in line with the present study, but the measured axial flux was almost parallel to the mean

flame brush and, therefore, is not suitable for assessing the present results, as noted above.

Third, as regards the other aforementioned DNSs, they dealt with decaying turbulence. Therefore, the transition from GD to CGT with flame development, observed in these studies, may, at least in part, be associated with a decrease in u'/S_L with time. To illustrate that turbulence decay is able to reverse transition from CGT to GD, we performed simulations by invoking time-dependent rms turbulent velocity and length scale

$$u'(t) = u'(t_0)\sqrt{\frac{t_0 + t_*}{t + t_*}} \qquad L^2(t) = C_d u' L(t + t_*) \qquad u'(t)L(t) = u'(t_0)L(t_0), \tag{30}$$

with t_* being evaluated using $L_0 \equiv L(t_0)$. If $t_0 = 0$ and $C_d = 0.5$, then $u'(t)/u'(t_0) = 0.6$ at $tu'(t_0)/L(t_0) = 3.6$ in line with the DNS data shown in Fig. 11 in the paper by Veynante et al. [15]. The results of the present simulations do indicate that transition from GD to CGT occurs in decaying turbulence (see bold lines and filled circles in Fig. 5a), with the transition time being strongly increased by $u'_0 \equiv u'(t_0)$ (cf. bold solid and dotted-dashed curves). Despite the transition reverses in decaying turbulence, (i) an increase in $N'_B = \tau S_L/u'_0$ still promotes CGT, i.e. reduces time required for the transition from GD to CGT (see Fig. 5b), in line with the experimental data discussed above, but (ii) θ_{tr} is not a single-valued function of N'_B

Finally, it is worth noting an interesting effect indicated by the 2D DNS by Veynante et al. [15]. Figure 10c from the cited paper shows CGT in the middle of

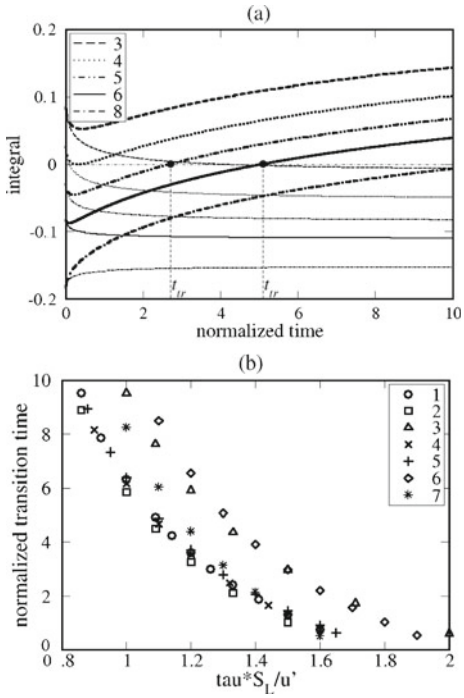

Fig. 5 **a** Dependencies of the integral given by Eq. 26 on the normalized flame development time $\theta = t/\tau_t$, calculated for decaying (*thick lines*) and frozen (*thin lines*) turbulence. A ratio of u'_0/S_L is specified in legends. Time is normalized using L_0 and u'_0. **b** Dependencies of normalized transition time on a ratio of $\tau S_L/u'$ calculated by varying either u' (1–3), or S_L (4–5), or τ (6–7). 1 - $S_L = 0.4$ m/s, $\tau = 6$; 2 - $S_L = 0.1$ m/s, $\tau = 6$; 3 - $S_L = 0.4$ m/s, $\tau = 3$; 4 - $u' = 1.5$ m/s, $\tau = 6$; 5 - $u' = 3.0$ m/s, $\tau = 6$; 6 - $u' = 0.8$ m/s, $S_L = 0.4$ m/s; 7 - $u' = 1.6$ m/s, $S_L = 0.4$ m/s

flame brush at $tu'_0/L_0 = 3.6$, while $\overline{\rho u'' c''} < 0$ everywhere at $tu'_0/L_0 = 4.2$. Definitely, such a transition from CGT to GD with time cannot be attributed to the decay of turbulence and the present authors are not aware of any explanation or even discussion of the emphasized phenomenon. It is encouraging that it is consistent with the present numerical data shown in Fig. 2. However, it would be optimistic to draw conclusions based on this single fact, especially as we did not observe such a transition when simulating decaying turbulence by invoking Eq. 30.

Although the present simulations indicate that transition from CGT to GD can occur in a developing flame that moves in a statistically stationary homogeneous turbulence, we do not claim that the opposite transition cannot occur in such a flame. The model Eq. 10 was developed by us [32] based on a theoretical consideration supplemented with a closure relation for a surface-conditioned correlation $(\overline{\mathbf{u}'_u \mathbf{n}'})_f$ between the flow velocity vector and the unit vector $\mathbf{n}$ normal to the infinitely thin instantaneous flame front (flamelet). The parameters of Eq. 11 were determined by simulating impinging-jet and statistically planar 1D flames [32, 33]. We are aware of a single paper [36] that reports the aforementioned correlation obtained in DNS in a single case. However, these DNS data do not allow us to draw a conclusion about eventual dependence of the correlation on flame-development time. Such a dependence could change the type (from CGT to GD or from GD to CGT) of the transition discussed. DNS research on the behavior of $(\overline{\mathbf{u}'_u \mathbf{n}'})_f$ in a developing premixed turbulent flame is strongly required to clarify the issue. Although the model addressed in the present work is consistent with currently available DNS and experimental data, future results could call for improvement of the model.

The transition type appears to depend substantially on a physical mechanism that controls the direction of turbulent scalar flux. If the preferential acceleration of light combustion products by the flame-induced mean pressure gradient is considered to be the primary cause of CGT [3, 20, 22], then, the transition from GD to CGT appears to occur during premixed turbulent flame development, as discussed in detail elsewhere [6]. This physical mechanism associated with large-scale processes was resolved in a LES study by Zimont and Battaglia [25] and caused the transition from GD to CGT in their simulations. However, there is another important physical mechanism, i.e. local flow acceleration due to the pressure drop in flamelets. This physical mechanism is a small-scale phenomenon and it was not addressed in the aforementioned LES study by Zimont and Battaglia [25]. Currently available numerical data (see Fig. 5 in Ref. [41] or Figs. 5 and 6 in Ref. [27]) indicate that both physical mechanisms play a substantial role, with the latter mechanism being of more importance at lower $\tilde{c}$ (cf. curves III and IV in Fig. 5 in Ref. [27]), shorter flame development times (cf. Fig. 5a and b in Ref. [27]), and smaller u'/S_L (cf. Figs. 5 and 6 in Ref. [27]).

The flow acceleration due to the pressure drop in flamelets could be responsible for occurrence of CGT during an early stage of premixed turbulent flame development. For instance, if we assume that the pressure gradient $(\nabla p)_f$ at a flamelet scales as $\tau S_L^2/\delta_L \mathbf{n}$, then, $(\overline{\partial p/\partial x})_f$ decreases as the flame develops, because $|\bar{n}_x| \approx 1$ initially when the flamelet is weakly wrinkled and is almost normal to the x-axis, but $|\bar{n}_x|$ decreases as the flamelet is wrinkled by turbulent eddies. Accordingly, the physical mechanism referred to appears to be of particular importance during an early stage of premixed turbulent flame development. It is worth stressing, however, that the model Eq. 10 does not straightforwardly address the aforementioned decrease in $|\bar{n}_x|$ with flame-development time.

Further research into the issue is definitely required. Nevertheless, we would like to stress that eventual transition from CGT to GD during premixed turbulent flame development has not yet been discussed in the literature to the best of the present authors' knowledge and this work is aimed, in particular, at drawing attention to this eventual phenomenon.

5 Conclusions

If the peak mean rate of product creation moves to the trailing edge of flame brush during development of a premixed flame that propagates in frozen turbulence, then, scalar flux can show the countergradient behaviour during an earlier stage of the flame development, followed by the transition to gradient diffusion at certain instant. In the case of decaying turbulence, transition can reverse, with GD (CGT) dominating during an earlier (later) stage of flame development, in line with available DNS data.

Both in frozen and decaying turbulence, transition instant depends strongly on turbulence and mixture characteristics. In particular, countergradient transport is suppressed by an increase in the rms turbulent velocity and by a decrease in the laminar flame speed or density ratio, in line with available experimental and DNS data.

The present simulations indicate that the peak mean rate of product creation is also shifted to the trailing edge of flame brush by an increase in u'/S_L and this observation offers an opportunity to explain the dependence of the direction of turbulent scalar flux on the Bray number in a hypothetical fully-developed flame.

The above trends lend qualitative support to the recent model of turbulent scalar flux given by Eqs. 10 and 11.

Acknowledgements The first author (AL) was supported by the Swedish Energy Agency and by the Chalmers Combustion Engine Research Center. (CERC). The second author (VS) was supported by ONERA.

References

1. Prudnikov, A.G.: Burning of homogeneous fuel-air mixtures in a turbulent flow. In: Raushenbakh, B.V. (ed.) Physical Principles of the Working Process in Combustion Chambers of Jet Engines, pp. 244–336. Clearing House for Federal Scientific & Technical Information, Springfield (1967)
2. Clavin, P., Williams, F.A.: Theory of premixed-flame propagation in large-scale turbulence. J. Fluid Mech. **90**, 589–604 (1979)
3. Libby, P.A., Bray, K.N.C.: Countergradient diffusion in premixed turbulent flames. AIAA J. **19**, 205–213 (1981)
4. Moss, J.B.: Simultaneous measurements of concentration and velocity in an open premixed turbulent flame. Combust. Sci. Technol. **22**, 119–129 (1980)
5. Tanaka, H., Yanagi, T.: Velocity-temperature correlation in premixed flame. Proc. Combust. Inst. **18**, 1031–1039 (1981)
6. Lipatnikov, A.N., Chomiak, J.: Effects of premixed flames on turbulence and turbulent scalar transport. Prog. Energy Combust. Sci. **36**, 1–102 (2010)
7. Kalt, P.A.M., Frank, J.H., Bilger, R.W.: Laser imaging of conditional velocities in premixed propane-air flames by simultaneous OH PLIF and PIV. Proc. Combust. Inst. **27**, 751–758 (1998)

8. Frank, J.H., Kalt, P.A.M., Bilger, R.W.: Measurements of conditional velocities in turbulent premixed flames by simultaneous OH PLIF and PIV. Combust. Flame **116**, 220–232 (1999)
9. Kalt, P.A.M., Chen, Y.C., Bilger, R.W.: Experimental investigation of turbulent scalar flux in premixed stagnation-type flames. Combust. Flame **129**, 401–415 (2002)
10. Troiani, G., Marrocco, M., Giammartini, S., Casciola, C.M.: Counter-gradient transport in the combustion of a premixed CH_4/air annular jet by combined PIV/OH-LIF. Combust. Flame **156**, 608–620 (2009)
11. Veynante, D., Piana, J., Duclos, J.M., Martel, C.: Experimental analysis of flame surface density models for premixed turbulent combustion. Proc. Combust. Inst. **26**, 413–420 (1996)
12. Most, D., Dinkelacker, F., Leipertz, A.: Direct determination of the turbulent flux by simultaneous application of filtered Rayleigh scattering thermometry and particle image velocimetry. Proc. Combust. Inst. **29**, 2669–2677 (2002)
13. Pfadler, S., Leipertz, A., Dinkelacker, F., Wäsle, J., Winkler, A., Sattelmayer, T.: Two-dimensional direct measurement of the turbulent flux in turbulent premixed swirl flames. Proc. Combust. Inst. **31**, 1337–1344 (2007)
14. Bray, K.N.C.: Turbulent transport in flames. Proc. R. Soc. Lond. A **451**, 231–256 (1995)
15. Veynante, D., Trouvé, A., Bray, K.N.C., Mantel, T.: Gradient and counter-gradient scalar transport in turbulent premixed flames. J. Fluid Mech. **332**, 263–293 (1997)
16. Veynante, D., Poinsot, T.: Effects of pressure gradients on turbulent premixed flames. J. Fluid Mech. **353**, 83–114 (1997)
17. Swaminathan, N., Bilger, R.W., Ruetsch, G.R.: Interdependence of the instantaneous flame front structure and the overall scalar flux in turbulent premixed flames. Combust. Sci. Technol. **128**, 73–97 (1997)
18. Louch, D.S., Bray, K.N.C.: Vorticity and scalar transport in premixed turbulent combustion. Proc. Combust. Inst. **27**, 801–810 (1998)
19. Chen, Y.C., Bilger, R.: Simultaneous 2–D imaging measurements of reaction progress variable and OH radical concentration in turbulent premixed flames: instantaneous flame-front structure. Combust. Sci. Technol. **167**, 187–222 (2001)
20. Zimont, V.L., Biagioli, F., Syed, K.: Modelling turbulent premixed combustion in the intermediate steady propagation regime. Prog. Comput. Fluid Dyn. **1**, 14–28 (2001)
21. Lipatnikov, A.N., Chomiak, J.: Developing premixed turbulent flames: part II. Pressure-driven transport and turbulent diffusion. Combust. Sci. Technol. **165**, 175–195 (2001)
22. Zimont, V.L., Biagioli, F.: Gradient, counter-gradient transport and their transition in turbulent premixed flames. Combust. Theor. Model. **6**, 79–101 (2002)
23. Biagioli, F., Zimont, V.L.: Gasdynamics modelling of counter-gradient transport in open and impinging turbulent premixed flames. Proc. Combust. Inst. **29**, 2087–2095 (2002)
24. Lipatnikov, A.N., Chomiak, J.: Self-similarly developing, premixed, turbulent flames: a theoretical study. Phys. Fluids **17**, 065105 (2005)
25. Zimont, V.L., Battaglia, V.: Joint RANS/LES approach to premixed flame modelling in the context of the TFC combustion model. Flow Turbulence Combust. **77**, 305–331 (2006)
26. Chakraborty, N., Cant, R.S.: Effects of Lewis number on scalar transport in turbulent premixed flames. Phys. Fluids **21**, 035110 (2009)
27. Lipatnikov, A.N.: Transient behavior of turbulent scalar transport in premixed flames. Flow Turbulence Combust. **86**, 609–637 (2011)
28. Trouvé, A., Poinsot, T.: Evolution equation for flame surface density in turbulent premixed combustion. J. Fluid Mech. **278**, 1–31 (1994)
29. Lipatnikov, A.N., Chomiak, J.: Turbulent flame speed and thickness: phenomenology, evaluation, and application in multi-dimensional simulations. Prog. Energy Combust. Sci. **28**, 1–74 (2002)
30. Lipatnikov, A.N.: Premixed turbulent flame as a developing front with a self-similar structure. In: Jiang, S.Z. (ed.) Focus on Combustion Research, pp. 89–141. Nova, New York (2006)
31. Lipatnikov, A.N.: Testing premixed turbulent combustion models by studying flame dynamics. Int. J. Spray Combust. Dynamics **1**, 39–66 (2009)
32. Sabelnikov, V.A., Lipatnikov, A.N.: A simple model for evaluating conditioned velocities in premixed turbulent flames. Combust. Sci. Technol. **183**, 588–613 (2011)
33. Sabelnikov, V.A., Lipatnikov, A.N.: Towards an extension of TFC model of premixed turbulent combustion. Flow Turbulence Combust. (2012). doi:10.1007/s10494-012-9409-9
34. Bray, K.N.C, Moss, J.B.: A unified statistical model for the premixed turbulent flame. Acta Astronaut. **4**, 291–319 (1977)
35. Driscoll, J.F.: Turbulent premixed combustion: flamelet structure and its effect on turbulent burning velocities. Prog. Energy Combust. Sci. **34**, 91–134 (2008)

36. Im, Y.H., Huh, K.Y., Nishiki, S., Hasegawa, T.: Zone conditional assessment of flame-generated turbulence with DNS database of a turbulent premixed flame. Combust. Flame **137**, 478–488 (2004)
37. Lipatnikov, A.N.: Conditionally averaged balance equations for modeling premixed turbulent combustion in flamelet regime. Combust. Flame **152**, 529–547 (2008)
38. Lipatnikov, A.N., Sabelnikov, V.A.: Exact solutions to reaction-diffusion equation and the direction of turbulent scalar flux in a premixed turbulent flame and its leading edge. In: Hanjalic, K., Nagano, Y., Borello, D., and Jakirlic, S. (eds.) THMT 12 Proceedings of the Seventh International Symposium Turbulence, Heat and Mass Transfer 7, University of Palermo, Italy, September 24–27, 2012, International Centre for Heat and Mass Transfer, CD, 2012, 13pp.
39. Lipatnikov, A.N., Sabelnikov, V.A.: Scalar flux at the leading edge of premixed turbulent flame brush (in preparation)
40. Domingo, P., Vervisch, L., Payet, S., Hauguel, R.: DNS of a premixed turbulent V flame and LES of a ducted flame using a FSD-PDF subgrid scale closure with FPI-tabulated chemistry. Combust. Flame **143**, 566–586 (2005)
41. Lipatnikov, A.N.: A test of conditioned balance equation approach. Proc. Combust. Inst. **33**, 1497–1504 (2011)